UNIVERSITÀ DEGLI STUDI DI TORINO

Multiple Exocytotic Markers Accumulate at the Sites of Perifungal Membrane Biogenesis in Arbuscular Mycorrhizas

A. Genre,S. Ivanov, M. Fendrych, A. Faccio, V. Žárský, T. Bisseling and P. Bonfante

Abstract

Arbuscular mycorrhizas (AMs) are symbiotic interactions established within the roots of most plants by soil fungi belonging to the Glomeromycota. The extensive accommodation of the fungus in the root tissues largely takes place intracellularly, within a specialized interface compartment surrounded by the so-called perifungal membrane, an extension of the host plasmalemma. By combining live confocal imaging of green fluorescent protein (GFP)-tagged proteins and transmission electron microscopy (TEM), we have investigated the mechanisms leading to the biogenesis of this membrane. Our results show that pre-penetration responses and symbiotic interface construction are associated with extensive membrane dynamics. They involve the main components of the exocytotic machinery, with a major participation of the Golgi apparatus, as revealed by both TEM and in vivo GFP imaging. The labeling of known exocytosis markers, such as v-SNARE proteins of the VAMP72 family and the EXO84b subunit of the exocyst complex, allowed live imaging of the cell components involved in perifungal membrane construction, clarifying how this takes place ahead of the growing intracellular hypha. Lastly, our novel data are used to illustrate a model of membrane dynamics within the pre-penetration apparatus during AM fungal penetration.

Key words: Daucus carota Exocytosis Medicago truncatula Membrane dynamics Plant–microbe interactions Symbiosis

Introduction

Arbuscular mycorrhizas (AMs) are symbiotic associations between Glomeromycota and the majority of plant species (Smith and Read 2008, Hata et al. 2010). These interactions develop in the rhizosphere, where signaling molecules released by both the plant and the fungus keep the respective partner informed of their reciprocal proximity and trigger pre-symbiotic responses ranging from gene regulation to metabolic changes, as well as morphogenetic events such as an increase in hyphal and root branching (Parniske 2008). Following this pre-symbiotic chemical dialog, a pivotal event in the establishment of AM interactions is the adhesion of a fungal hyphopodium to the host root epidermis (Bonfante and Genre 2008). Direct physical contact, in fact, marks the initiation of the symbiotic phase and represents the first step towards the colonization of inner root tissues. Root colonization is characterized by the development of intracellular fungal structures, including the highly branched arbuscules where the exchange of mineral nutrients for photosynthesis-derived carbohydrates takes place. All intracellular fungal structures are accommodated inside a novel cell compartment, called the symbiotic interface. It is composed of plant cell wall materials and bordered by an extension of the host plasma membrane (Parniske 2008, Genre and Bonfante 2010).

We have shown that hyphopodium contact causes an impressive reorganization of the epidermal cell cytoplasm, leading to the appearance of a novel structure, the so-called pre-penetration apparatus, or PPA (Genre et al. 2005). This is a broad, columnar aggregation of cytoplasm that predicts the future track of the penetrating hypha through the epidermal cell lumen. A few similarities have been found between the PPA and the infection thread (IT), induced by symbiotic nitrogen-fixing rhizobia (Gage 2004). Remarkably, the processes of PPA and IT assembly are strictly controlled, in legumes, by the 'common SYM' pathway, a signal transduction pathway that mediates the intracellular accommodation of both AM fungi and rhizobia (Oldroyd and Downie 2006). Pre-penetration responses are not limited to legumes. The observation of PPAs in Daucus carota (a plant belonging to the Asterales, which are phylogenetically very distant from the Leguminosae) suggests that pre-penetration responses are shared among AM hosts (Genre et al. 2008), and have probably been conserved from the common ancestors that first established a symbiotic association with glomeromycetes, at least 400 Mya, in the early Devonian (Redecker et al. 2000).

Furthermore, pre-penetration responses are not restricted to epidermal cells but extend to all root cells that undergo AM colonization. Broad PPAs are organized in cortical cells, associated with arbuscule development (Genre et al. 2008). Such a reoccurrence of the pre-penetration response whenever new intracellular hyphae develop strongly suggests that the PPA has a role in fungal accommodation inside the host cells.

From this perspective, the composition of the PPA, which has been partially elucidated, gives clear indications. Beside the nucleus, whose movements to and from the fungal contact site are associated with the initiation and full development of the PPA, the cytoplasmic aggregate includes thick bundles of cytoskeletal fibres and an extensive proliferation of endoplasmic reticulum (ER). Electron microscopy investigations have also shown an abundance of Golgi stacks as well as trans-Golgi vesicles and tubules (Genre et al. 2008). Equally, Golgi stack accumulation has also been observed around young arbuscules (Pumplin and Harrison 2009). All of these observations suggest the presence of secretory activity inside the PPA, which has therefore been proposed to have a function in the assembly of the perifungal membrane, the extension of the plant plasma membrane that envelopes each intracellular hypha, maintaining host cell integrity. This has only been postulated so far on the basis of indirect evidence: (i) the PPA anticipates the intracellular fungal route; (ii) PPA dismantling is associated with the appearance of the perifungal

membrane; (iii) PPA-like aggregates are also observed in advance of arbuscule branch development; and (iv) plant mutants for SYM pathway genes, where PPA assembly is hampered, are not successfully colonized by AM fungi.

The aim of the reported research is to investigate how the perifungal membrane is built inside the PPA. For this, we have expressed different green fluorescent protein (GFP) constructs in two model plants, the legume Medicago truncatula and the non-legume D. carota, by Agrobacterium rhizogenes-mediated root transformation. We have tagged the main elements of the secretory pathway, including the Golgi apparatus and proteins involved in the fusion of secretory vesicles with their target membranes [SNARE (soluble N-ethylmaleimide-sensitive factor attachment protein receptor) proteins of the vesicle-associated membrane protein 72 (VAMP72) family and a member of the exocyst complex]. Our results show that such cell components and proteins accumulate inside the PPA aggregate, indicating the onset of a major exocytotic event a short distance from the growing hyphal tip, and strongly suggesting this as the site of perifungal membrane assembly.

Results

GFP:MAN-labeled compartments accumulate inside the PPA

In order to assist the reader in interpreting our images, two pictures of PPAs where the ER is labeled by GFP–HDEL (Genre et al. 2005, Genre et al. 2008) are presented in Supplementary Fig. 1. Beside being interpreted as a putative marker of exocytotic activity since it was first observed (Parniske 2008), the intense accumulation of GFP-labeled ER highlights very clearly the PPA outline, making it easier to read the images obtained with the other GFP markers presented in this work.

The expression of GFP:MAN (a fusion of GFP with α-1,2 mannosidase I; Nebenführ et al. 1999) in D. carota resulted in a bright labeling of spot-like compartments, dispersed in the cytoplasm, as shown in Fig. 1A and B for differentiated epidermal cells. Such organelles are interpreted as cis-Golgi elements according to Nebenführ et al. (1999). Occasionally, a weak labeling of the ER and particularly the nuclear envelope was also visible in these lines, probably related to the synthesis of the chimeric proteins in the ER lumen prior to their accumulation in the cis-Golgi.

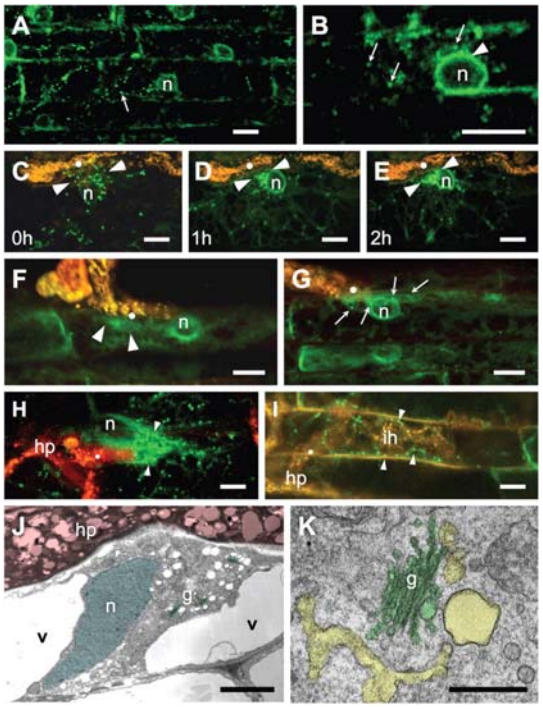

Fig. 1 Organization of the Golgi apparatus in D. carota during the pre-penetration response. Labeling of the Golgi apparatus by GFP:MAN inside epidermal cells from control roots grown in the absence of the AM fungus is shown in A and B. Several Golgi stacks (arrows) are visible as bright dots spread across the cytoplasm. The expression of this construct also displays a weak labeling of the nuclear envelope (B, arrowhead), marking the position of the nucleus (n). (C–E) Time series covering 2 h of observation and showing the progressive accumulation of Golgi stacks in the PPA area (arrowheads) between the nucleus (n) and contact point (•). (F and G). Golgi stack dynamics upon fungal contact as analyzed through the acquisition of a single focal plane at 1.6 s intervals over 2 min (the corresponding videos are presented as Supplementary Movies 1 and 2, respectively). Image averaging displays green halos in those areas where the GFP:MAN fluorescence has been recorded more often during the observation time. In both images, the brightest areas are associated with the contact point (•) and perinuclear cytoplasm (n). Furthermore, the permanence of a few Golgi stacks within the PPA area is highlighted in G by the presence of isolated green spots (arrows), corresponding to single stacks that have remained still over most of the acquisition time. (H) Persistence of Golgi stack accumulation during fungal penetration. A penetration hypha developing from a hyphopodium (hp) has entered the epidermal cell through the initial contact point (•) and is developing within the PPA area (arrowheads). A large number of Golgi stacks accumulate in the PPA between the penetrating hypha and the nucleus (n). (I) Epidermal cell traversed by an intracellular hypha (ih) that has developed from the hyphopodium (hp) through the contact point (•). Scattered Golgi stacks (arrowheads) are visible in the cytoplasm surrounding the hypha. (J and K) Transmission electron micrographs showing Golgi stacks inside a PPA. (J) The cytoplasmic aggregation, positioned underneath a contacting hyphopodium (hp, red) and crossing the vacuole (v), includes the nucleus (n, blue) and several Golgi stacks (g, green). (K) A higher magnification shows a single Golgi stack (g, green) associated with extensive trans-Golgi membranes (yellow). Bars: (A–I) 20 µm; (J) 5 µm; (K) 0.5 µm.

Upon hyphopodium adhesion to an epidermal cell (Fig. 1C–E), a progressive accumulation of GFP:MAN bodies could be observed in the vicinity of the contact site, corresponding to the PPA area (compare with Supplementary Fig. 1).

Golgi stacks are extremely motile organelles in the plant cell, where they display rapid movements along the F-actin/ER network (Nebenführ et al. 1999). For this reason, visualizing them in still images is not by itself very informative regarding their activity. We therefore acquired several time-lapse movies, recording a frame every 1.6 s over 2 min intervals. The resulting animations show the rapid dynamics of the Golgi

apparatus, both in control roots and in the presence of the AM fungus (Supplementary Movies 1–3). To obtain a global view of the dynamics of the Golgi apparatus, we have then used Leica Confocal Software to prepare averaged images from each time-lapse movie. Such images show bright areas in those regions where the GFP-labeled Golgi stacks have passed more often or have stayed for longer, during the 2 min observation. As represented in Fig. 1F and G (corresponding to Supplementary Movie 1 and 2, respectively), a diffuse fluorescence was observed in the perinuclear cytoplasm, where Golgi stacks often pass. Significantly, blurred areas of green fluorescence could also be clearly seen in the PPA area, in the vicinity of the hyphopodium contact site. Furthermore, a few bright spots could often be observed in the PPA area, indicating that a few GFP:MAN compartments have remained still during most of the observation time. Apart from the perinuclear region, areas and spots of comparable brightness were not observed in control cells from uninfected roots (Supplementary Fig. 2). Upon fungal penetration of the epidermal cell, a dense accumulation of GFP-labeled Golgi stacks can still be observed in the part of the PPA that is located ahead of the growing hyphal tip (Fig. 1H); in contrast, after PPA dismantling, GFP:MAN compartments distribute along the intracellular hypha with a much lower density (Fig. 1I). The abundance of Golgi stacks in the PPA aggregate was also confirmed by transmission electron microscopy (TEM) analyses, where several piles of Golgi cisternae were detected (Fig. 1J), associated with an extensive tubular–vesicular trans-Golgi network (Fig. 1K).

Taken together, these observations indicate that Golgi stacks accumulate inside the PPA volume, where they also spend a relatively longer time compared with the rest of the cytoplasm. Such a concentration of the Golgi apparatus activity in the PPA fits in with the activation of the plant secretory pathway before and during fungal penetration of the epidermal cell.

VAMP72 marks the site of perifungal membrane biogenesis

Membrane fusion in eukaryotic cells is regulated by specific proteins known as SNAREs (Brunger 2006). SNARE-mediated membrane fusion is achieved by the formation of a highly stable protein association named the SNARE complex. A typical SNARE complex involves three distinct types of proteins residing on the target membrane (t-SNARE) and one protein located on the transport vesicle (v-SNARE) that together contribute to a four-helix bundle of intertwined SNARE domains (Brunger 2006). Since VAMPs of the VAMP72 family are v-SNAREs known to be involved in secretory processes (Sanderfoot 2007, Kwon et al. 2008a), we chose three constructs where the GFP was fused to VAMP721a, VAMP721d and VAMP721e. By screening their distribution in the root cells, we observed that all VAMP fusions marked cell division sites inside the meristems of M. truncatula (Fig. 2A, Supplementary Fig. 3A, B), as well as the tips of growing root hairs (Fig. 2B, Supplementary Fig. 3E, F).

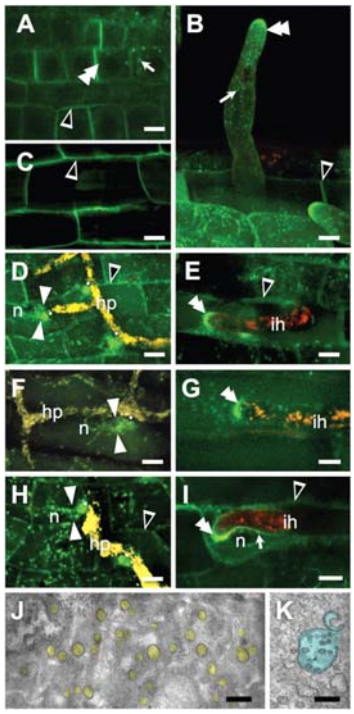

Fig. 2: GFP tagging of VAMP72 proteins in M. truncatula highlighting vesicle accumulation and perifungal membrane proliferation inside the PPA. (A–C) Pattern of GFP:VAMP721e localization in the root meristem (A), atrichoblastic (B) and trichoblastic epidermal cells (C). In addition to a number of punctate cytoplasmic bodies (arrows), and a weaker signal along the plasma membrane (black arrowheads), fluorescence mainly accumulated along the newly laid cell walls (double arrow) of meristematic cells (A) and in the root hair tip (double arrows) of trichoblasts (B), indicating the recruitment of VAMP72 proteins in the root major exocytotic events. (D–I) Subcellular localization of GFP:VAMP721a (D, E), GFP:VAMP721d (F, G) and GFP:VAMP721e (H, I) upon hyphopodium (hp) contact (D, F, H) and cell entry (E, G, I). In analogy to uninfected roots, a weak fluorescence was observed along the plasma membrane (black arrow) only for VAMP721a (D, E) and VAMP721e (H, I). The three constructs gave rise to an intense fluorescence within the PPA area (arrowheads), generally more focused towards the contact site (•) than the nucleus (n). After cell entry, a crescent-shaped pattern (double arrow) embracing the tip of the intracellular hypha (ih) was observed in the three lines. This distribution of fluorescence is likely to derive from the accumulation of GFP-tagged vesicles and their fusion into the developing perifungal membrane. The latter was more extensively labeled by GFP:VAMP721e (I, arrow). Furthermore, fluorescent punctate bodies were often observed in the PPA area and throughout the cytoplasm (evident in D, G and H). (J and K) Transmission electron micrographs of the PPA aggregate, showing the abundance of vesicles (J, yellow) and MVB (K, blue). Bars: (A–I) 20 µm; (J, K) 0.5 µm.

Minor differences could be detected in the distribution pattern of each construct. Cell division sites and root hair tips were the only detectable targets of GFP:VAMP721d (Supplementary Fig. 3B, D, F). In contrast, fluorescence was also detected in the plasma membrane of both meristematic and differentiated cells from the lines expressing GFP:VAMP721a (Supplementary Fig. 3A, C) and GFP:VAMP721e (Fig. 2A–C), reflecting the retention of the proteins on the target membrane, possibly due to the saturation of the exocytotic pathway by overexpression. Small punctate cytoplasmic bodies were often found also to be labeled by the three VAMP72 constructs (Fig. 2, Supplementary Fig. 3).

The VAMP72 constructs therefore proved to be reliable markers of exocytosis in M. truncatula root organ cultures (ROCs) as already described in Arabidopsis (Kwon et al. 2008a, Kwon et al. 2008b).

Hyphopodium development on the surface of an epidermal cell induced an accumulation of fluorescence in the vicinity of the contact site, suggesting the local concentration of GFP-tagged secretory vesicles (Fig 2D, F, H). This condition is also supported by electron microscopy images, showing broad clusters of vesicles inside the PPA (Fig. 2J).

Later, after fungal penetration, the fluorescence concentrated in the vicinity of the growing hyphal tip (Fig. 2E, G, I) and its position could be deduced based on the cytosolic autofluorescence of Gigaspora gigantea. Such a pattern, which can derive from the GFP tagging of VAMP72 proteins in both the secretory vesicles and the membrane where they have just fused, revealed the site of perifungal membrane proliferation.

Also in this condition, the three VAMP72 proteins displayed minor but significant differences in their localization patterns. GFP:VAMP721a (Fig. 2E) and GFP:VAMP721d (Fig. 2G) were concentrated in the shape of a crescent, just ahead of the growing hyphal tip. In addition to this localization, GFP:VAMP721e also marked part of the perifungal membrane on the side of the hypha, up to 40–50 µm from the tip (Fig. 2I). Both before and after fungal penetration, moving punctate bodies were constantly labeled in the cytoplasm by the three constructs. Interestingly, TEM images of the PPA aggregate show abundant late endosomes [or multivesicular bodies (MVBs)], as shown in Fig. 2K.

Perifungal membrane proliferation involves the exocyst complex

Throughout eukaryotes, vesicle targeting is mediated by a hetero-oligomeric protein complex known as the exocyst, tethering the vesicle to its target membrane prior to SNARE involvement and membrane fusion (Hála et al. 2008, Fendrych et al. 2010). We therefore chose the EXO84 subunit of the exocyst complex as a further marker of exocytotic activity (Guo et al. 1999). GFP-tagged AtEXO84b produced a comparable labeling in both D. carota (Fig. 3A, B) and M. truncatula (Fig. 3C, D), with a moderate but selective labeling of the young root hair tips (Fig. 3A, B). In particular, the apical dome was marked by the fluorescent signal only in the root hair tips that were rich in cytoplasm, a hallmark of active tip growth, whereas the GFP fluorescence was absent in vacuolated hairs, where growth is arrested (Fig. 3C, D).

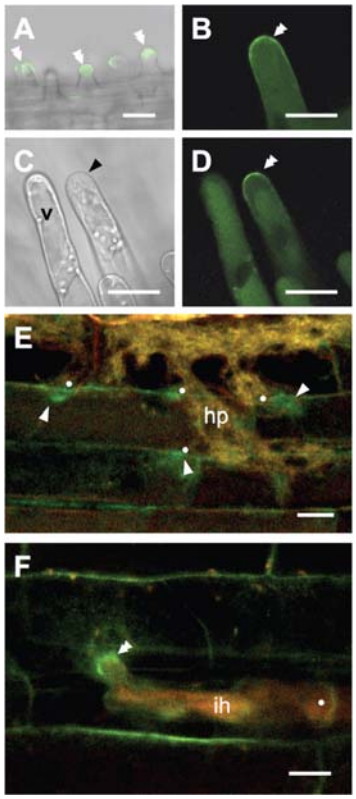

Fig. 3 Tagging of exocytotic sites with GFP:EXO84b in D. carota and M. truncatula. (A and B) The expression of GFP:EXO84b in control roots of carrot clearly labeled the tips of growing root hairs (double arrows). A superimposition of GFP fluorescence and bright-field is presented in A, whereas a higher magnification of the fluorescence image alone is shown in B. (C and D) An analogous pattern was observed in M. truncatula. Comparing the bright-field image in C with the fluorescence in D shows that the fluorescent signal (double arrow) is restricted to the growing, cytoplasm-rich hair tip (black arrowhead), whereas a nearby vacuolated root hair (v) is unlabeled, indicating that EXO84b is recruited by the secretory machinery of tip growth. (E) In the presence of a G. gigantea hyphopodium (hp) a diffuse fluorescence appears in the PPAs (arrowheads), adjacent to the contact sites (•). (F) Upon fungal penetration (•), fluorescence concentrates in a crescent-shaped pattern (double arrow) associated with the tip of the intracellular hypha (ih). Bars: (A–D) 30 μm; (E, F) 20 μm.

Significantly, GFP:EXO84b accumulated underneath G. gigantea hyphopodia (Fig. 3E), highlighting the PPA aggregate with a diffuse signal. During intracellular fungal development, the construct labeled a crescent shape encompassing the growing hyphal tip (Fig. 3F).

In conclusion, the constitutive expression of fluorescently labeled AtEXO84b in both D. carota and M. truncatula selectively marked the growing root hair tips and the area of the developing perifungal membrane, indicating the involvement of the exocyst complex in both processes. In addition, the visualization of GFP:EXO84b around the tip of intracellular hyphae confirmed that the perifungal membrane develops inside the PPA, a short distance ahead of the growing hyphal tip, as already suggested by VAMP constructs.

Membrane dynamics in arbuscule development

The small diameter of carrot roots also allowed the visualization of GFP:MAN and GFP:EXO84b in the root inner tissues. The accumulation of Golgi stacks that was described during pre-penetration responses in epidermal cells was also observed in the inner root cortex of D. carota, associated with developing intracellular hyphae (Fig. 4A, B). In contrast, cells where an arbusculated coil had fully developed had a much lower density of labeled Golgi bodies (Fig. 4B). A precise labeling by GFP:EXO84b was observed only around the tips of developing intracellular hyphae (Fig. 4C) and branches (Fig. 4D, E), whereas fully differentiated arbuscules were not associated with any signal (Fig. 4E), indicating the involvement of the exocyst complex in the proliferation of the periarbuscular membrane. Interestingly, GFP:EXO84b also marked the sites where a hyphal tip crossed a plant cell wall (Fig. 4C), suggesting an additional role for the exocyst in the fusion between the perifungal membrane and the plasmalemma upon fungal exit from the cell.

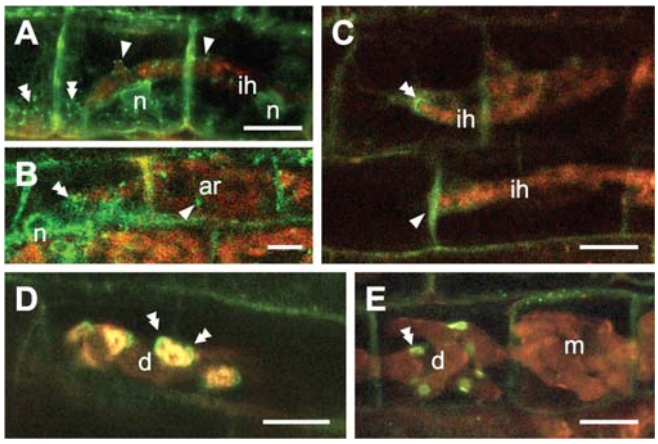

Fig. 4 Perifungal membrane biogenesis in the inner cortex of D. carota roots. (A and B) Labeling of the Golgi apparatus by GFP:MAN. Several Golgi stacks (double arrows) clustered ahead of growing intracellular hyphae (orange), whereas isolated stacks (arrowheads) distributed along the sides of fully grown intracellular hyphae (ih) and arbuscules (ar). (C–E) Similar to what was observed in epidermal cells, GFP:EXO84b labeled the proliferating perifungal membrane with crescent-shaped patterns (double arrows) associated with the tip of intracellular hyphae (C, ih) and developing (d) arbuscule branches (D, E). No signal was associated with mature arbuscules (m), suggesting that the exocyst involvement is limited to the phase of membrane proliferation. Furthermore, an accumulation of fluorescence was also observed in the sites where hyphae crossed plant cell walls (C, arrowhead), hinting at a possible role for the exocyst complex in the membrane dynamics associated with hyphal exit from the host cell. Bars: 20 μm.

Discussion

To investigate the process of perifungal membrane synthesis, we developed ROCs from the legume M. truncatula and the non-legume D. carota, two established models for the study of AM interactions. The two species give complementary advantages for cell biology investigations: while the large cells of M. truncatula can be of help in visualizing the precise subcellular location of the fluorescent constructs, carrot has finer roots which are more amenable to TEM protocols and also allow an easier visualization of the inner root tissues by confocal microscopy.

Although our use of constitutive promoters hampers the direct deduction of a role for the VAMP72 family and exocyst complex in the pre-penetration responses, the fact that all the exocytotic markers that we

were able to test were recruited to the fungal penetration site/PPA strongly suggests that this is a major exocytotic event, comparable in intensity with cell plate deposition, apical growth or polarized defense against pathogens.

Furthermore, by labeling functional markers of the exocytotic process such as VAMP72 proteins and the exocyst complex, we were able to visualize indirectly the formation of the perifungal membrane inside the PPA in living root cells. In our observations, in fact, a crescent-shaped structure is constantly observed ahead of the growing intracellular hyphae. This pattern may derive either from the retention of GFP-tagged proteins in the newly formed perifungal membrane (probably due to their overexpression) or from the accumulation of secretory vesicles around the membrane. Combined with fungal autofluorescence, this gave rise to a negative staining for the space comprised between the perifungal membrane and the hypha (interface compartment). We can therefore deduce that the perifungal membrane surrounding the symbiotic interface assembles a short distance ahead of the growing hyphal tip, resembling the development of the IT membrane ahead of the file of rhizobia inside a root hair (Fournier et al. 2008).

Our observations provide direct support for a model of symbiotic interface assembly (Fig. 5), where the required elements of the endomembrane system concentrate at the contact site and along the future route of the intracellular hypha, contributing to the PPA aggregate; vesicle fusion on the plasma membrane facing the penetration site is then proposed to initiate the inward membrane proliferation that associates with fungal penetration and is maintained during the subsequent intracellular hyphal growth.

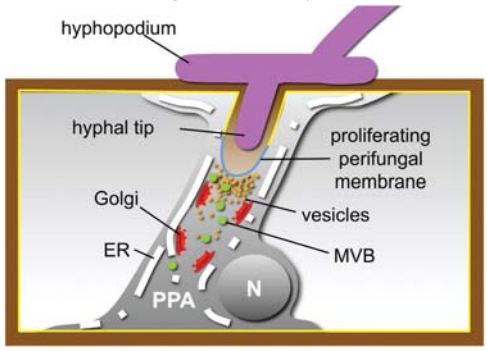

Fig. 5 Proposed model of perifungal membrane biogenesis in AMs. The scheme represents intracellular fungal development in an epidermal cell, reporting the localization of the developing perifungal membrane and different components of the secretory pathway within the pre-penetration apparatus (PPA). ER, endoplasmic reticulum; MVB, multivesicular body; N, nucleus.

Perifungal membrane biogenesis in AMs as an exocytotic process

The assembly of an interface compartment, surrounded by a host-derived membrane, is a constant feature in biotrophic interactions. Intracellular extensions of the plasma membrane or large plasmalemma-derived vesicles are found around symbiotic bacteria such as rhizobia (Brewin 2004), endomycorrhizal fungi (Hata et al, 2010) and pathogenic fungi or oomycetes (O'Connell and Panstruga 2006). Increasing evidence indicates that the de novo synthesis of such biotrophic interfaces derives from focal targeting of secretory vesicles (Takemoto et al. 2003, Micali et al. 2010), although this may give rise to membrane protrusions either around the neck (Kankanala et al. 2007) or at the tip of the penetrating hypha (Micali et al. 2011). Generally speaking, biotrophic interfaces are more extended in symbiotic than in pathogenic interactions

(An et al. 2006). While the biotrophic growth of filamentous pathogens is often limited to single cells, root infection by nitrogen-fixing bacteria extends throughout the root tissues, with a few similarities to the AM colonization process (Gage 2004). Rhizobia proceed along the IT, a tubular invagination of the plant plasma membrane which envelops a filamentous colony of bacteria (Fournier et al. 2008). ITs develop from one cell to the next and can also branch as they cross the root outer and inner cell layers. Plant cell wall matrix components are found in the IT lumen (Berry et al. 2002, Tsyganova et al. 2009), suggesting that its biogenesis involves exocytosis. Along the same lines, basic components of the plant cell wall have been localized in the thin space that runs between the fungal wall and the perifungal membrane (Balestrini and Bonfante 2005). Taken together, these features suggest exocytosis to be a central process in interface biogenesis also for AM interactions.

Our present results provide direct support for this hypothesis indicating an exocytosis-driven proliferation of the perifungal membrane in the vicinity of hyphal tips. We show that all the elements of the plant secretory pathway accumulate inside the PPA, in strict relation to the process of cell entry by the AM fungus. The ER cisternae expand and Golgi apparatus activity concentrates in the cytoplasmic aggregate that marks the intracellular fungal route. Three v-SNARE proteins of the VAMP72 family and a component of the exocyst concentrate in the PPA cytoplasm, indicating this as a site of intense exocytosis, as previously shown in the case of growing pollen tube tips (Hála et al. 2008, Fendrych et al. 2010). Although possibly deriving from the artificial overexpression of the constructs, and even if we could not discriminate between the direct labeling of the membrane or just the adjacent secretory vesicles, both VAMP72 and exocyst constructs allowed the visualization of the perifungal membrane proliferation process in vivo, showing that this takes place ahead of penetrating and intracellularly growing hyphal tips.

Involvement of the secretory pathway in AM interactions

The reorganization of the Golgi apparatus in arbusculated cells has already been observed by Pumplin and Harrison (2009). Their description of clustered Golgi bodies around the branches of active arbuscules resembles our observations of Golgi stack distribution around intracellular hyphae and young arbuscules, while we did not observe as many Golgi bodies around the mature arbusculated coils of carrot. This suggests that the high dynamicity of the Golgi apparatus may in fact result in different pictures when single snapshots of the organization of a cell are recorded, which was the case for both investigations: while Pumplin and Harrison (2009) have analyzed sectioned samples, we were observing untouched, living roots, but the intensity of the laser radiation required for recording a single z-axis series quickly exhausted the GFP fluorescence, hampering adequate time-lapse acquisitions. Furthermore, it is possible that the terminal arbuscules of M. truncatula observed by Pumplin and Harrison (2009) and the intercalary arbusculated coils of carrot that we show in the present study undergo slightly different developmental processes. It has to be noted anyway that the density of Golgi stacks was much higher in the PPA-related cytoplasmic aggregates than in the cytoplasm from any of the colonized cells. This hints at a major role for the Golgi apparatus in the pre-penetration response, with particular reference to the development of the interface matrix and membrane.

Interestingly, frequent passages and relative immobility of the Golgi bodies have been reported in pathogen-induced cytoplasmic aggregations, such as those that Arabidopsis epidermal cells develop in response to Peronospora parasitica attacks (Takemoto et al. 2003). The same authors report the proliferation of ER cisternae in the same area, and we have shown (Genre et al. 2009) that ER accumulation in M. truncatula, in response to mycorrhizal but also to biotrophic and necrotrophic pathogenic fungi, depends on the functionality of DMI3, a central element of the SYM pathway that also controls rhizobium

colonization in legumes. Furthermore, Golgi proliferation (Koh et al. 2005) and the involvement of some of the v-SNARE proteins that we have analyzed, such as VAMP721a and VAMP721d (Lipka and Panstruga 2005, Kwon et al. 2008a, Kwon et al. 2008b, Frei dit Frey and Robatzek 2009), have been described in Arabidopsis responses to powdery mildews. Similarly, exocyst subunits have been shown to be involved in plant pathogenic interactions (Chong et al. 2009, Pečenková et al. 2011).

On the one hand, these results suggest that—at least on a mechanistic basis—some of the plant cell responses to pathogenic and symbiotic microbes can be compared. Both types of interactions activate the secretory pathway and focus it at the contact/penetration site. On the other hand, such comparable secretory mechanisms obviously deliver different combinations of materials to the apoplast. Both responses lead to the deposition of new cell wall components, but at least in the case of incompatible pathogenic interactions, such molecules (which include suberin, lignins and similar resistant polymers) are firstly reinforcing the wall to build a physical barrier against invasion (O'Connell and Panstruga 2006). In contrast, in the case of symbionts, the soft newly laid cell wall constitutes the niche where the microorganism is going to develop (Genre and Bonfante 2005). The fact that defense-related compounds are not reported to be released in the presence of AM fungi and rhizobia seems to support this hypothesis, indicating a markedly differential use of the secretory machinery by the plant cell, depending on the nature of the interacting microbe.

The sustained membrane flux required for perifungal membrane proliferation in AMs is not unidirectional. The frequent observation of late endosomes in TEM images of the PPA (as shown in Fig. 2K) suggest, on the one hand, that the punctate bodies labeled by the VAMP constructs could indeed be endosomes, probably involved in the recycling of the v-SNAREs back from the plasma membrane. On the other hand, such observations confirm the simultaneous presence of exo- and endocytosis, an acknowledged feature common to all major secretory events.

Beside the recycling of surplus membrane, endosomes can be directly involved in signaling (Geldner and Robatzek 2008). This possibility is particularly intriguing in AM interactions, where a lot of attention is currently being focused on the signaling molecules (Maillet et al. 2011) and signal transduction mechanisms (Chabaud et al. 2011) that mediate fungal recognition by the host plant. Although the study of signal exchange within the interface remains at present out of our reach, it will be important to investigate whether pre-symbiotic signaling in the rhizosphere and post-contact interface biogenesis are mediated by the same mechanisms. In this respect, evidence is emerging of a role for AM fungal effector proteins (Kloppholtz et al. 2011), similar to what occurs in pathogenic interactions, and important clues about their delivery to the plant cell can come from the comparison of membrane dynamics before and after fungal contact.

Materials and Methods

Construct integration in A. rhizogenes

All of the constructs used for this study were GFP fusions expressed in plants under the constitutive promoters 35S from Cauliflower mosaic virus (35SCaMV) or Arabidopsis Ubiquitin3 (UBQ). To visualize the ER (Haseloff et al. 1997), the GFP was fused to the signal peptide HDEL, causing the chimeric protein to accumulate inside the ER lumen. Transformed ROCs expressing this construct were already available and had been used for previous studies (Genre et al. 2008). In GFP:MAN the GFP is fused to the α-1,2

mannosidase I gene. Since the encoded protein accumulates in cis-Golgi cisternae, this construct was used to visualize Golgi stacks inside the plant cytoplasm (Nebenführ et al. 1999). In this case, competent A. rhizogenes cells (strain Ar1193) were transfected by electroporation according to Dower et al. (1988) with a suspension of pBIN20 vector carrying the GFP:MAN construct (kindly provided by Andreas Nebenführ, University of Colorado, USA). Briefly, an 80 µl suspension of electrocompetent A. rhizogenes (strain Ar1193) was added with 2 µl of 40 ng ml−1 plasmid solution in ultrapure water and incubated on ice for 1 min. The suspension was then transferred to the cuvette of a MicroPulser Electroporator (Biorad) and pulsed at 2.5 kV according to the manufacturer's instructions. After the addition of 300 µl of SOC medium, bacteria were incubated for 1 h at 37°C and plated on selective LB medium. After incubation at 28°C during 48 h, one of the kanamycin-resistant colonies was then subcultured and used for plant transformation. The GFP:EXO84b construct is a fusion of GFP with the EXO84b component of the exocyst, a protein complex made up of at least eight subunits, which is involved in tethering secretory vesicles to their target membranes during polar exocytosis (Fendrych et al. 2010). The construct, inserted in a pK7FWG2 vector, was introduced into Ar1193 A. rhizogenes by electroporation as described above, except that the transformed colonies were selected against spectinomycin before being used for plant transformation. In GFP:VAMP721a (formerly 7-3 or 72-1), GFP:VAMP721d (7-4 or 72-2) and GFP:VAMP721e (7-5 or 72-3) the GFP is fused to the coding sequences of three different VAMP family members and those were expressed under the UBQ promoter.

Plant and fungal materials

Medicago truncatula genotype Jemalong A17 and the horticultural D. carota var. sativus were used in this study. Agrobacterium rhizogenes-transformed ROCs expressing the different GFP constructs were obtained according to Boisson-Dernier et al. (2001) for M. truncatula and according to Bécard and Fortin (1988) for carrot. Transformed roots with a high level of fluorescence were selected 21 d after inoculation, decontaminated and subcultured on M medium at 25°C in the dark for subsequent use as ROCs. GFP:MAN was only expressed in carrot, the three VAMP72 constructs were expressed in M. truncatula, while GFP:EXO84b lines were produced in both plants.

The AM fungus used in this study was G. gigantea isolate HC/FE30 (Herbarium Cryptogamicum Fungi, University of Torino, Italy), which is characterized by a strong cytoplasmic autofluorescence (Séjalon-Delmas et al. 1998).

To obtain mycorrhizal interactions in vitro, spores were pre-germinated, placed in Petri dishes with fresh root cultures and covered with 25 µm Lumox film (Dutscher SAS), as described in Genre et al. (2008). Medicago truncatula ROCs were grown in vertically oriented Petri dishes to favor the development of a regular fishbone-shaped root system (Chabaud et al. 2002). The non-gravitropic carrot ROCs were initially grown horizontally and then switched to vertical growth following fungal inoculation in order to facilitate hyphal targeting of young lateral roots. Petri dishes were visually screened to detect highly ramifying hyphae and root–fungus contacts, which were then examined by confocal and electron microscopy.

Confocal microscopy

A Leica TCS-SP2 confocal microscope was used for all the experiments described in this work. GFP fluorescence was excited using the 488 nm line of the argon laser and recorded at 500–525 nm. Gigaspora gigantea autofluorescence was excited with the same laser band and acquired at 570–700 nm. A scanning

resolution of 1,024 × 1,024 pixels was chosen and serial optical sections were acquired with 1 or 2 µm resolution along the z-axis. Bright-field images were acquired simultaneously using the transmission detector of the microscope. For each transformed line, a minimum of 10 independent roots was examined. In all cases the living roots were observed untouched, using the Lumix film as a coverslip, inside the Petri dish into which the roots were grown, taking advantage of a long-distance ×40 water immersion objective (Leica HCX Apo 0.80). In the case of the GFP:MAN lines, Golgi stack movements were recorded by time-lapse acquisitions at 1.6 s intervals for 2 min, using the same imaging conditions.

Electron microscopy

Samples for TEM were processed as described in Genre et al. (2008). Briefly, root segments were fixed in 2% glutaraldehyde, post-fixed in 1% OsO4, stained with aqueous 0.5% uranyl acetate and then dehydrated in an ascending series of ethanol to 100% followed by absolute acetone. Samples were then infiltrated in Epon–Araldite (Hoch 1986) resin and flat-embedded (Howard and O'Donnell 1987). The resin was polymerized for 24 h at 60°C. Embedded samples were processed for ultramicrotomy: semi-thin sections (0.5 mm) were stained with 1% toluidine blue, and ultra-thin (70 nm) sections were counter-stained with uranyl acetate and lead citrate (Reynolds 1963). These were used for TEM analyses under a Philips CM10 transmission electron microscope.

Funding

This work was supported by the University of Turin [fondi ex 60% 2008]; the Italian National Project PRIN 2008; Regione Piemonte [CIPE-BioBITs]; the Czech Science Foundation [GACR_P305/11/1629]; Ministry of Education, Youth and Sports (MSMT) [MSM0021620858]; the Netherlands Organization for Scientific Research (NWO); Russian Federation for Basic Research [grant for Centre of Excellence (RFFI) 047.018.001].

Acknowledgments

We are grateful to Elena Fedorova and Erik Limpens for their help with the VAMP72 constructs and critical revision of the text; to Andreas Nebenführ for kindly providing the GFP:MAN construct; to Mireille Chabaud for the GFP–HDEL construct; and to David Barker for fruitful discussion.

References

An Q, Huckelhoven R, Kogel KH, van Bel AJE. Multivesicular bodies participate in a cell wall-associated defence response in barley leaves attacked by the pathogenic powdery mildew fungus. Cell. Microbiol. 2006;8:1009-1019.

Balestrini R, Bonfante P. The interface compartment in arbuscular mycorrhizae: a special type of plant cell wall? Plant Biosyst. 2005;139:8-15.

Bécard G, Fortin JA. Early events of vesicular-arbuscular mycorrhiza formation on Ri T-DNA transformed roots. New Phytol. 1988;108:211-218.

Berry AM, Rasmussen U, Bateman K, Huss-Danell K, Lindwalland S, Bergman B. Arabinogalactan proteins are expressed at the symbiotic interface in root nodules of Alnus spp. New Phytol. 2002;155:469-479.

Boisson-Dernier A, Chabaud M, Garcia F, Becard G, Rosenberg C, Barker DG. Agrobacterium rhizogenes-transformed roots of Medicago truncatula for the study of nitrogen-fixing and endomycorrhizal symbiotic associations. Mol. Plant-Microbe Interact. 2001;14:695-700.

Bonfante P, Genre A. Plants and arbuscular mycorrhizal fungi: an evolutionary–developmental perspective. Trends Plant Sci. 2008;13:492-498.

Brewin NJ. Plant cell wall remodelling in the Rhizobium–legume symbiosis. Crit. Rev. Plant Sci. 2004;23:293-316.

Brunger AT. Structure and function of SNARE and SNARE-interacting proteins. Q. Rev. Biophys. 2006;38:1-47.

Chabaud M, Venard C, Defaux-Petras A, Bécard G, Barker D. Targeted inoculation of Medicago truncatula in vitro root cultures reveals MtENOD11 expression during early stages of infection by arbuscular mycorrhizal fungi. New Phytol. 2002;156:265-273.

Chabaud M, Genre A, Sieberer BJ, Faccio A, Fournier J, Novero M, et al. Arbuscular michorrizal hyphopodia and germinated spore exudates trigger Ca2+ spiking in the legume and nonlegume root epidermis. New Phytol. 2011;189:347-355.

Chong YT, Gidda SK, Sanford C, Parkinson J, Mullen RT, Goring DR. Characterization of the Arabidopsis thaliana exocyst complex gene families by phylogenetic, expression profiling, and subcellular localization studies. New Phytol. 2009;185:401-419.

Dower WJ, Miller JF, Ragsdale CW. High efficiency transformation of E. coli by high voltage electroporation. Nucleic Acids Res. 1988;16:6127-6145.

Fendrych M, Synek L, Pečenková T, Toupalová H, Cole R, Drdová E, et al. The Arabidopsis exocyst complex is involved in cytokinesis and cell plate maturation. Plant Cell 2010;22:3053-3065.

Fournier J, Timmers AC, Sieberer BJ, Jauneau A, Chabaud M, Barker DG. Mechanism of infection thread elongation in root hairs of Medicago truncatula and dynamic interplay with associated rhizobial colonization. Plant Physiol. 2008;148:1985-1995.

Frei dit Frey N, Robatzek S. Trafficking vesicles: pro or contra pathogens? Plant Biol. 2009;12:437-443.

Gage DJ. Infection and invasion of roots by symbiotic, nitrogen-fixing Rhizobia during nodulation of temperate legumes. Microbiol. Mol. Biol. Rev. 2004;68:280-300.

Geldner N, Robatzek S. Plant receptors go endosomal: a moving view on signal transduction. Plant Physiol. 2008;147:1565-1574.

Genre A, Bonfante P. The making of symbiotic cells in arbuscular mycorrhizal roots. In: Koltai H, Kapulnik Y, editors. Arbuscular Mycorrhizas: Physiology and Function. 2nd edn. The Netherlands: Springer, Dordrecht; 2010. p. 57-71.

Genre A, Chabaud M, Faccio A, Barker DG, Bonfante P. Prepenetration apparatus assembly precedes and predicts the colonization patterns of arbuscular mycorrhizal fungi within the root cortex of both Medicago truncatula and Daucus carota. Plant Cell 2008;20:1407-1420.

Genre A, Chabaud M, Timmers T, Bonfante P, Barker DG. Arbuscular mycorrhizal fungi elicit a novel intracellular apparatus in Medicago truncatula root epidermal cells before infection. Plant Cell 2005;17:3489-3499.

Genre A, Ortu G, Bertoldo C, Martino E, Bonfante P. Biotic and abiotic stimulation of root epidermal cells reveals common and specific responses to arbuscular mycorrhizal fungi. Plant Physiol. 2009;149:1424-1434.

Guo W, Grant A, Novick P. Exo84p is an exocyst protein essential for secretion. J. Biol. Chem. 1999;274:23558-23564.

Hála M, Cole R, Synek L, Drdová E, Pecenkova T, Nordheim A, et al. An exocyst complex functions in plant cell growth in arabidopsis and tobacco. Plant Cell 2008;20:1330-1345.

Haseloff J, Siemering KR, Prasher DC, Hodge S. Removal of a cryptic intron and subcellular localization of green fluorescent protein are required to mark transgenic Arabidopsis plants brightly. Proc. Natl Acad. Sci. USA 1997;94:2122-2127.

Hata S, Kobae Y, Banba M. Interactions between plants and arbuscular mycorrhizal fungi. Int. Rev. Cell Mol. Biol. 2010;281:1-48.

Hoch HC. Freeze-substitution of fungi. In: Aldrich HC, Todd WJ, editors. Ultrastructure Techniques of Microorganisms. New York: Plenum Press; 1986. p. 183-211.

Howard RJ, O'Donnell KL. Freeze substitution of fungi for cytological analysis. Exp. Mycol. 1987;11:250-269.

Kankanala P, Czymmek K, Valent B. Roles for rice membrane dynamics and plasmodesmata during biotrophic invasion by the blast fungus. Plant Cell 2007;19:706-724.

Kloppholz S, Kuhn H, Requena N. A secreted fungal effector of glomus intraradices promotes symbiotic biotrophy. Curr. Biol. 2011;21:1204-1209.

Koh S, Andre A, Edwards H, Ehrhardt D, Somerville S. Arabidopsis thaliana subcellular responses to compatible Erysiphe cichoracearum infections. Plant J. 2005;44:516-529.

Kwon C, Bednarek P, Schulze-Lefert P. Secretory pathways in plant immune responses. Plant Physiol. 2008b;147:1575-1583.

Kwon C, Neu C, Pajonk S, Yun HS, Lipka U, Humphry M, et al. Co-option of a default secretory pathway for plant immune responses. Nature 2008a;451:835-840.

Lipka V, Panstruga R. Dynamic cellular responses in plant–microbe interactions. Curr. Opin. Plant Biol. 2005;8:625-631.

Maillet F, Poinsot V, André O, Puech-Pagès V, Haouy A, Gueunier M, et al. Fungal lipochitooligosaccharide symbiotic signals in arbuscular mycorrhiza. Nature 2011;469:58-63.

Micali CO, Neumann U, Grunewald D, Panstruga R, O'Connell R. Biogenesis of a specialized plant–fungal interface during host cell internalization of Golovinomyces orontii haustoria. Cell. Microbiol. 2011;13:210-226.

Nebenführ A, Gallagher LA, Dunahay TG, Frohlick JA, Mazurkiewicz AM, Meehl JB, et al. Stop-and-go movements of the plant Golgi stacks are mediated by the acto-myosin system. Plant Physiol. 1999;121:1127-1141.

O'Connell RJ, Panstruga R. Tête à tête inside a plant cell: establishing compatibility between plants and biotrophic fungi and oomycetes. New Phytol. 2006;171:699-718.

Oldroyd G, Downie A. Nuclear calcium changes at the core of symbiosis signaling. Curr. Opin. Plant Biol. 2006;9:351-357.

Parniske M. Arbuscular mycorrhiza: the mother of plant root endosymbioses. Nat. Rev. Microbiol. 2008;6:763-775.

Pečenková T, Hála M, Kulich I, Kocourková D, Drdová E, Fendrych M, et al. The role for the exocyst complex subunits Exo70B2 and Exo70H1 in the plant–pathogen interaction. J. Exp. Bot. 2011;62:2107-2016.

Pumplin N, Harrison MJ. Live-cell imaging reveals periarbuscular membrane domains and organelle location in Medicago truncatula roots during arbuscular mycorrhizal symbiosis. Plant Physiol. 2009;151:809-819.

Redecker D, Kodner R, Graham LE. Glomalean fungi from the Ordovician. Science 2000;289:1920-1921.

Reynolds EW. The use of lead citrate at high pH as an electron opaque stain in electron microscopy. J. Cell Biol. 1963;17:208-212.

Sanderfoot A. Increases in the number of SNARE genes parallels the rise of multicellularity among the green plants. Plant Physiol. 2007;144:6-17.

Séjalon-Delmas N, Magnier A, Douds DD, Bécard G. Cytoplasmic autofluorescence of an arbuscular mycorrhizal fungus Gigaspora gigantea and nondestructive fungal observations in planta. Mycologia 1998;90:921-926.

Smith SE, Read DJ. Mycorrhizal Symbiosis. New York: Academic Press; 2008.

Takemoto D, Jones DA, Hardham AR. GFP-tagging of cell components reveals the dynamics of subcellular re-organization in response to infection of Arabidopsis by oomycete pathogens. Plant J. 2003;33:775-792.

Tsyganova AV, Tsyganov VE, Findlay KC, Borisov AY, Tikhonovich IA, Brewin NJ. Distribution of legume arabinogalactan protein-extensin (AGPE) glycoproteins in symbiotically defective pea mutants with abnormal infection threads. Cell Tissue Biol. 2009;3:93-102